Quantum Electronics **43** (1) 90–93 (2013)

LASER METHODS IN BIOLOGY

PACS numbers: 87.64.Cc; 42.62.Be
DOI: 10.1070/QE2013v043n01ABEH014968

Laser beam scattering on an inhomogeneous ensemble of elliptical discs modelling red blood cells in an ectacytometer

S.Yu. Nikitin, M.A. Kormacheva, A.V. Priezzhev, A.E. Lugovtsov

Abstract. **We have theoretically studied the effect of difference in particle shapes on the appearance of the diffraction pattern, which arises in the scattering of a laser beam on a dilute suspension of erythrocytes in an ectacytometer. We have proposed data processing algorithms allowing one to estimate the red blood cell shape parameter variance under conditions of laser ectacytometry. The conclusions of the theoretical analysis are verified experimentally.**

Keywords: *diffraction, laser, particle, erythrocyte, deformability, ectacytometer, elliptical disc, spread of particle shapes, shear stress.*

1. Introduction

The flow of blood through small blood vessels (capillaries) is highly dependent on the deformability of erythrocytes, i.e., the ability of red blood cells to change their shape under the action of external forces and shear stresses. One of the methods of experimental research of deformability of red blood cells outside the body (*in vitro*) is laser ectacytometry that relies on the use of viscous friction forces and diffraction of light [1]. When illuminating a small amount of red blood cells in the suspension, a diffraction pattern appears on the observation screen located in the far-field zone, which contains information about the shape of the particles under study.

In the population of red blood cells of a healthy and especially a sick person, various cells have, in general, different ability to deform. This allows us to consider the deformability as a statistical characteristic of an ensemble of particles and to use for its description such notions as the distribution function, the mean and the variance.

The purpose of this paper is to analyse analytically the effect of differences in the shapes of the particles deformed due to a shear stress on the appearance of the diffraction pattern observed in the case of laser diffractometry of red blood cells, as well as to verify experimentally the conclusions of the theoretical analysis.

S.Yu. Nikitin, M.A. Kormacheva Department of Physics, M.V. Lomonosov Moscow State University, Vorob'evy gory, 119991 Moscow, Russia; e-mail: sergeynikitin007@yandex.ru, kormacheva.marie@gmail.com;
A.V. Priezzhev Department of Physics, M.V. Lomonosov Moscow State University, Vorob'evy gory, 119991 Moscow, Russia; International Laser Center, M.V. Lomonosov Moscow State University, Vorob'evy gory, 119991 Moscow, Russia; e-mail: avp2@mail.ru; avp2@phys.msu.ru;
A.E. Lugovtsov International Laser Center, M.V. Lomonosov Moscow State University, Vorob'evy gory, 119991 Moscow, Russia; e-mail: anlug@tut.by

Received 4 July 2012; revision received 17 September 2012
Kvantovaya Elektronika **43** (1) 90–93 (2013)
Translated by I.A. Ulitkin

2. Principle of ectacytometer operation

In an ectacytometer, the erythrocyte suspension is placed into a gap between the walls of two transparent coaxial discs or cylindrical glasses, one of which is fixed and the other can be rotated at a variable speed (so-called Couette cell)*. The rotation of the movable glass causes the fluid flow and the appearance of shear stresses that deform red blood cells. In Couette flow, the shear rate and shear stress, which is proportional to this rate, are constant along the radial coordinate at a fixed speed of the cylinder rotation. In some (limited from above) range of shear stresses and in the absence of interaction between the particles (which is typical for dilute suspensions) the deformable cells become stretched and oriented along the fluid flow. To monitor the changes in the particle shape, the erythrocyte suspension is probed with a laser beam. The ectacytometer provides the conditions for single scattering, which can be easily achieved by diluting appropriately the investigated cell suspension with a saline.

Note that in the case of a standard suspension concentration, instantaneously about a thousand of cells are illuminated by the laser beam in the gap of the Couette cell, with some cells being constantly replaced by the others moving in the flow. This leads to an averaging of the observed diffraction pattern with respect to the cell population.

Generally, in the case of normal blood, the diffraction pattern contains a central intensity maximum and a few barely visible interference lines, which are similar in shape to the circles in the absence of shear stresses and to ellipses, if there are any [1]. This indicates that normal red blood cells in the flow acquire a shape similar to ellipsoidal one. The diffraction pattern is recorded with a video camera and transmitted to the computer. A special code makes it possible to observe on the monitor the points with the same intensity of light. Commonly for this purpose use is made of the boundary of the central diffraction maximum (i.e., the first minimum of the diffraction pattern), which is approximated with an ellipse. The ratio of the semiaxes of the ellipse as a function of the shear rate (or shear stress) in the Couette cell characterises the average red blood cell deformability, which is measured in these experiments.

3. Red blood cell model

We model a red blood cell by a transparent elliptical disk, i.e., a cylinder whose bottom is formed by an ellipse. The model

* For definiteness, in what follows we will discuss the variant with a cylindrical Couette cell.

relies on the images of red blood cells in a shear flow, obtained by microscopy and shown in Fig. 1 [2, 3]. Another argument in favour of our model is the proximity of the scattering phase function from biconcave and flat disks, calculated in the discrete-dipole approximation for small angles. The lengths of the semiaxes of the elliptic disk a and b are assumed to be random variables:

$$a = a_0(1 + \varepsilon), \quad b = b_0(1 - \varepsilon),$$

where a_0 and b_0 are the average lengths of the semiaxes and ε is a random parameter (the particle shape parameter). We assume that the average value of the shape parameter is equal to zero: $\langle\varepsilon\rangle = 0$, and its variance is $\langle\varepsilon^2\rangle \equiv \mu^2 \ll 1$. Thus, the inhomogeneity of the ensemble with respect to the shape of the particles is weak. In addition, $ab \approx a_0 b_0$, i.e., the elliptical discs have approximately the same surface areas and volumes, but different eccentricity.

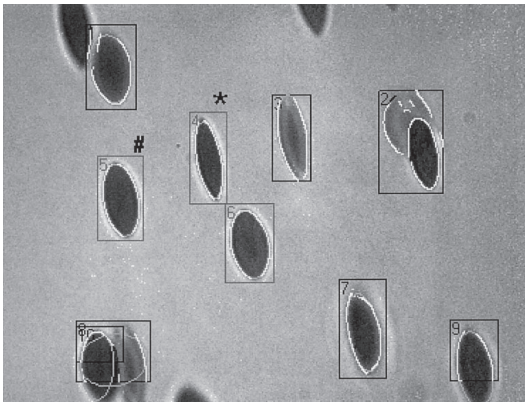

Figure 1. Microscopic images of red blood cells in a shear flow [2, 3].

4. Results

Using the approach developed in our papers [4–6], we obtained an approximate analytical expression for the distribution of light intensity on the observation screen near the central maximum of the diffraction pattern. It has the form

$$f \equiv \frac{1}{4\beta^2}\frac{I}{I(0)} = (1 - r)^2 + \mu^2\cos^2 2\varphi. \qquad (1)$$

Here I is the intensity of the scattered light and $I(0)$ is the intensity in the central maximum of the diffraction pattern. Polar coordinates r and φ are given by

$$\frac{x}{A} = r\cos\varphi, \quad \frac{y}{B} = r\sin\varphi, \qquad (2)$$

where x and y are the Cartesian coordinates of points on the observation screen; $A = q_1 z/(ka_0)$ and $B = q_1 z/(kb_0)$ are the parameters determining the size of the diffraction pattern (i.e., the distance from the centre of the pattern to the first diffraction minimum); z is the distance from the volume under study to the observation screen; $k = 2\pi/\lambda$ is the wave number; and λ is the wavelength of light. Constants q_1 and β are the parameters of the Bessel function and are defined by the formulas $q_1 = 3.82 = \text{const}$, $\beta = -0.4 = \text{const}$. In deriving (1) we assumed that the bases of elliptical discs lie in the same plane, perpendicular to the laser beam axis. This is in agreement with experimental observations.

Note that the origin of the coordinates lies at the centre of the diffraction pattern. The x axis is directed horizontally and the y axis – vertically, with one of the axis being parallel to the direction of the flow in the Couette cell, and with the other being perpendicular to it.

5. Characteristics of the diffraction pattern

To interpret the experimental data obtained by laser diffractometry of erythrocytes, we introduce some new concepts, such as skeletal curve, polar curve, polar intensity, dark points, light points, characteristic points. Let us give their definitions.

A skeletal curve is the locus of points on the observation screen, at which the light intensity as a function of distance from the point to the centre of the diffraction pattern reaches a minimum for the first time. This curve can be found on the observation screen in the case of both a homogeneous and an inhomogeneous ensemble of particles. The difference lies in the fact that for a homogeneous ensemble of particles the skeletal curve is the iso-intensity curve, and for an inhomogeneous ensemble, the light intensity will not be the same at various points on the skeletal curve.

An iso-intensity curve is a curve on the observation screen, on which the intensity of light is constant.

Dark points are the points of the skeletal curve, at which the light intensity reaches a minimum and becomes equal to zero.

Polar (light) points are the points of the skeletal curve, at which the light intensity reaches a maximum.

Polar intensity is the minimum light intensity, at which the iso-intensity curve covers the centre of the diffraction pattern.

A polar curve is an iso-intensity curve passing through polar points. In the experiment, the polar curve can be found as the curve of the minimum constant light intensity, covering the centre of the diffraction pattern.

Characteristic points are the points, at which the radius vectors of the dark points intersect the polar curve.

Using formulas (1) and (2) it is easy to obtain the equations of the skeletal and polar curves and, also, to determine the coordinates of dark, light and characteristic points. The equation of the skeletal curve has the form $r = 1$, or

$$\frac{x^2}{A^2} + \frac{y^2}{B^2} = 1.$$

Thus, the skeletal curve is an ellipse with semiaxes A and B. Note that this curve would comprise the first minimum of the diffraction pattern in the absence of a spread in the particle shapes (when $\mu = 0$). The ratio of the semiaxes of the skeletal curve is equal to the ratio of the sizes of average semiaxes of the elliptical discs: $A/B = b_0/a_0$. The distribution of the normalised intensity of light on the skeletal curve is described by the expression

$$f_s = \mu^2\cos^2 2\varphi. \qquad (3)$$

The equation of an iso-intensity curve has the form $r = 1 \pm \sqrt{f - \mu^2\cos^2 2\varphi}$. The lowest light intensity, at which the iso-intensity curve is closed and covers the centre of the diffraction pattern is given by the formula $f_p = \mu^2$, or

$$\frac{1}{4\beta^2}\frac{I_p}{I(0)} = \mu^2, \qquad (4)$$

where I_p is the polar intensity. The same light intensity I_p will be on the polar curve, which actually represents the boundary of the central maximum of the diffraction pattern. According to formula (4), this boundary will be the lighter, the greater the inhomogeneity of the ensemble of particles.

The equation of the polar curve has the form

$$r(\varphi) = 1 - \mu|\sin 2\varphi|, \tag{5}$$

or, in the Cartesian coordinates,

$$\begin{aligned} x(\varphi) &= A(1 - \mu|\sin 2\varphi|)\cos\varphi, \\ y(\varphi) &= B(1 - \mu|\sin 2\varphi|)\sin\varphi. \end{aligned} \tag{6}$$

The dark points have the coordinates $x_d = \pm A/\sqrt{2}$ and $y_d = \pm B/\sqrt{2}$. These expressions follow from formulas (2) for $r = 1$ and $\varphi = \pi/4 + n\pi/2$, where $n = 0, 1, 2, \ldots$. The dark points form vertices of a rectangle on the observation screen. The aspect ratio of the rectangle is equal to the ratio of the lengths of the average semiaxes of the elliptical discs: $x_d/y_d = b_0/a_0$. According to our model, the intensity of light in the dark points must be equal to zero.

The light (polar) points have the coordinates $x_p = 0$, $y_p = \pm B$ and $x_p = \pm A$, $y_p = 0$. These points lie at the intersections of the polar curve with the axes of the coordinates and form the vertices of a rhombus. The coordinates of characteristic points are as follows: $x_c = (1 - \mu)(A/\sqrt{2})$, $y_c = (1 - \mu)(B/\sqrt{2})$.

The skeletal curve, dark and polar points are presented in Fig. 2. This figure also shows the polar curve and characteristic points. Note that the shape of the polar curve is very close to the shape of the iso-intensity curve obtained in [7], where the method of laser diffraction was used to study the erythrocyte suspension containing normal cells and cells with reduced deformability. This fact can be considered as an experimental confirmation of our model.

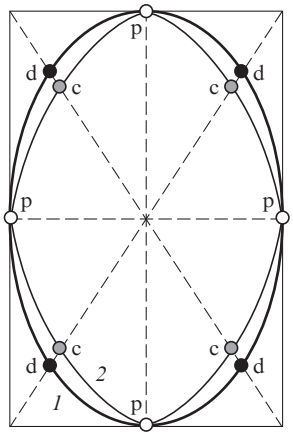

Figure 2. (*1*) Skeletal and (*2*) polar curves, (d) dark, (p) polar and (c) characteristic points. The polar curve is constructed by formula (6) for $\mu = 0.1$.

The existence of four dark points on the boundary of the central diffraction maximum, which form the vertices of a rectangle can be regarded as an indicator of the inhomogeneity of the ensemble with respect to the shapes (the degree of elongation) of the cells.

The curves and points we introduced into consideration can be found in the diffraction pattern.

6. Methods for estimating the particle shape parameter variance

The particle shape parameter variance can be determined by the characteristics of the polar curve, dark, light and characteristic points. Here are several ways to estimate the parameter μ from the experimental data obtained by the method of laser diffractometry.

The parameter μ can be estimated by making use of the light intensity in the polar points

$$\mu^2 = 1.5 I_p/I(0), \tag{7}$$

by making use of the coordinates of dark and characteristic points

$$\mu = 1 - l_c/l_d, \tag{8}$$

by making use of the coordinates of characteristic points

$$\mu = 1 - l_c \frac{\sqrt{2}}{\sqrt{A^2 + B^2}}, \tag{9}$$

by making use of the direction of the tangent to the polar curve at the polar point

$$\mu = \frac{A}{2B}\tan\chi, \tag{10}$$

where l_c is the distance from the centre of the diffraction pattern to the characteristic points; l_d is the distance from the centre of the diffraction pattern to the dark point; and χ is the angle between the vertical and the tangent to the polar curve at the polar point.

Finally, the particle shape parameter variance can be determined directly by means of formulas (6). In the latter case μ should be considered as a fitting parameter of the theoretical model. The value of μ must be sought from the condition of the best fit of the shapes of the experimental iso-intensity curve and polar curve.

More accurate estimates can be obtained by numerical calculation of the diffraction patterns and more sophisticated models of red blood cells. To this end, use can be made of the discrete-dipole [8] and ray-wave [9, 10] approximations.

7. Experimental study of an inhomogeneous ensemble of red blood cells

The data presented in Fig. 2 show that when a laser beam is scattered on a homogeneous ensemble of deformed red blood cells, the boundary of the central diffraction maximum should have an elliptical shape (the skeletal curve in Fig. 2). If an ensemble of red blood cells contains cells of different shapes, the boundary of the central diffraction maximum acquires not an elliptical, but, for example, a diamond shape (polar curve in Fig. 2). To verify the conclusions of our model, we conducted an experiment on scattering of a laser beam on the erythrocyte suspension containing cells of different shapes. In this experiment, we used rat erythrocytes. We prepared an erythrocyte suspension, which contained equal amounts of the two cell types: normal (deformable) red blood cells and

red blood cells with reduced deformability. The latter were obtained by treating the cells with a solution of glutaraldehyde. The photograph of the diffraction pattern is shown in Fig. 3b. For comparison, Fig. 3a shows a photograph of the diffraction pattern observed in the scattering of the laser beam on the suspension of normal (deformable) rat erythrocytes. One can see that in Fig. 3a the boundary of the central diffraction maximum is elliptical, and in Fig. 3b it is diamond-shaped. Thus, the experimental data confirm the main conclusions of our theoretical model.

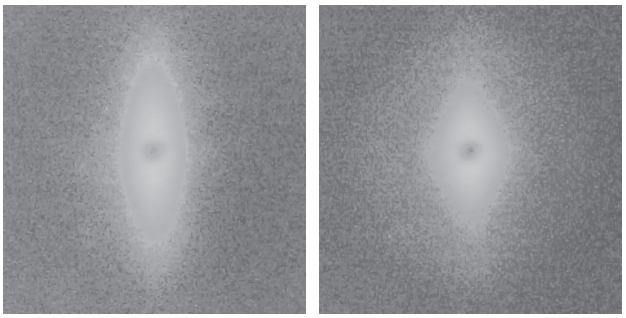

a b

Figure 3. Photographs of the diffraction patterns obtained with a laboratory ectacytometer in the scattering of the laser beam on suspensions of different rat erythrocytes: (a) normal (deformable) erythrocytes and (b) a mixture of normal (deformable) and non-deformable erythrocytes at a ratio of 1:1.

8. Conclusions

We have considered the effect of different shapes (the degree of elongation) of the particles on the appearance of the diffraction pattern produced in the scattering of a laser beam on a dilute suspension of erythrocytes in an ectacytometer. An analytical expression has been derived for the light intensity distribution in the diffraction pattern near the central diffraction maximum. We have established the relation between the erythrocyte shape parameter variance and the characteristics of the observed diffraction pattern. The algorithms have been proposed to process the experimental data obtained by laser diffractometry, allowing one to estimate the erythrocyte shape parameter variance in the suspension under study.

According to our calculations, the diffraction pattern, arising in the scattering of a laser beam on an inhomogeneous ensemble of red blood cells in the single-scattering regime, should have special characteristics. An indicator of the inhomogeneity of the ensemble with respect to the particle shapes can be the presence of four dark points, which form the vertices of a rectangle, on the boundary of the central diffraction maximum. The lighter the boundary of the central diffraction maximum (i.e., the higher the intensity of light on the polar curve), the greater the inhomogeneity of the ensemble of particles. Another indicator of the inhomogeneity of the ensemble of erythrocytes with respect to the particle shapes is the fact that the boundary of the central maximum of the diffraction pattern becomes diamond shaped. These and other features make it possible to quantify such a population characteristic as the erythrocyte shape parameter variance.

Usually an ectacytometer measures the average deformability of erythrocytes in a blood sample. We believe that it can also be used to measure the variance of the red blood cell deformability. To do this, it is needed to measure the light intensity distribution along straight lines passing through the centre of the diffraction pattern (we call them intersecting lines). The most important are the horizontal and vertical lines, and the lines passing through the dark and the characteristic points of the diffraction pattern.

Acknowledgements. This work was partially supported by the Russian Foundation for Basic Research (Grant No. 12-02-01329-a).

References

1. Mohandas N., Clark M.R., Jacobs M.S., Shohet S.B. *J. Clin. Invest.*, **66**, 563 (1980).
2. Dobbe J.G.G., Hardeman M.R., Streekstra G.J., Strackee J., Ince C., Grimbergen C.A. *Blood Cells, Molecules, and Diseases*, **28** (3), 373 (2002).
3. Dobbe J.G.G., Streekstra G.J., Hardeman M.R., Ince C., Grimbergen C.A. *Cytometry (Clinical Cytometry)*, **50**, 313 (2002).
4. Nikitin S.Yu., Priezzhev A.V., Lugovtsov A.E., in *Advanced Optical Flow Cytometry: Methods and Disease Diagnoses*. Ed. by V.V. Tuchin (Weinheim: Wiley-VCH, 2011) pp 133–154.
5. Nikitin S.Yu., Lugovtsov A.E., Priezzhev A.V. *Kvantovaya Elektron.*, **40** (12), 1074 (2010) [*Quantum Electron.*, **40** (12), 1074 (2010)].
6. Nikitin S.Yu., Lugovtsov A.E., Priezzhev A.V. *Kvantovaya Elektron.*, **41** (9), 843 (2011) [*Quantum Electron.*, **41** (9), 843 (2011)].
7. Streekstra G.J., Dobbe J.G.G., Hoekstra A.G. *Opt. Express*, **18** (13), 14173 (2010).
8. Yurkin M.A., Maltsev V.P., Hoekstra A.G. *J. Quant. Spectrosc. Radiat. Transfer*, **106**, 546 (2007).
9. Priezzhev A.V., Nikitin S.Yu., Lugovtsov A.E. *J. Quant. Spectrosc. Radiat. Transfer*, **110**, 1535 (2009).
10. Lugovtsov A.E., Nikitin S.Yu., Priezzhev A.V. *Kvantovaya Elektron.*, **38** (6), 606 (2008) [*Quantum Electron.*, **38** (6), 606 (2008)].